Title

Giant clam growth in the Gulf of Aqaba is accelerated compared to fossil populations

Journal

Proceedings of the Royal Society B, 288(1957)

ISSN

0962-8452

Authors

Killam, Daniel
Al-Najjar, Tariq
Clapham, Matthew

Publication Date

2021-08-25

DOI

10.1098/rspb.2021.0991

Peer reviewed

PROCEEDINGS B

royalsocietypublishing.org/journal/rspb

Research

Cite this article: Killam D, Al-Najjar T, Clapham M. 2021 Giant clam growth in the Gulf of Aqaba is accelerated compared to fossil populations. *Proc. R. Soc. B* **288**: 20210991.
https://doi.org/10.1098/rspb.2021.0991

Received: 27 April 2021
Accepted: 5 August 2021

Subject Category:
Palaeobiology

Subject Areas:
environmental science, palaeontology

Keywords:
sclerochronology, *Tridacna*, stable isotopes, conservation palaeobiology

Author for correspondence:
Daniel Killam
e-mail: daniel.e.killam@gmail.com

Electronic supplementary material is available online at https://doi.org/10.6084/m9.figshare.c.5565670.

THE ROYAL SOCIETY PUBLISHING

Giant clam growth in the Gulf of Aqaba is accelerated compared to fossil populations

Daniel Killam[1], Tariq Al-Najjar[2] and Matthew Clapham[1]

[1]Department of Earth and Planetary Sciences, University of California, Santa Cruz, CA, USA
[2]Department of Marine Biology, University of Jordan, Aqaba Branch, Jordan

DK, 0000-0001-7569-1828; MC, 0000-0003-4867-7304

The health of reef-building corals has declined due to climate change and pollution. However, less is known about whether giant clams, reef-dwelling bivalves with a photosymbiotic partnership similar to that found in reef-building corals, are also threatened by environmental degradation. To compare giant clam health against a prehistoric baseline, we collected fossil and modern *Tridacna* shells from the Gulf of Aqaba, Northern Red Sea. After calibrating daily/twice-daily growth lines from the outer shell layer, we determined that modern individuals of all three species (*Tridacna maxima*, *T. squamosa* and *T. squamosina*) grew faster than Holocene and Pleistocene specimens. Modern specimens also show median shell organic $\delta^{15}N$ values 4.2‰ lower than fossil specimens, which we propose is most likely due to increased deposition of isotopically light nitrate aerosols in the modern era. Nitrate fertilization accelerates growth in cultured *Tridacna*, so nitrate aerosol deposition may contribute to faster growth in modern wild populations. Furthermore, colder winter temperatures and past summer monsoons may have depressed fossil giant clam growth. Giant clams can serve as sentinels of reef environmental change, both to determine their individual health and the health of the reefs they inhabit.

1. Introduction

Giant clams are distributed throughout the tropical Indo-Pacific [1], but the coral reefs they inhabit are in crisis due to the combined stress of climate change and pollution, particularly from nitrate-mediated eutrophication [2]. In the central Red Sea, coral growth has slowed since the 1970s, largely attributed to heat stress [3], despite suggestions that the Red Sea is a putative refuge for corals in the face of climate change [4]. While anthropogenic change has only recently affected mean sea surface temperature (SST) in the Red Sea, seasonality was greater in the last interglacial (Late Pleistocene, 125 ka) and Holocene (4–6 ka), resulting in reduced coral growth rates at that time [5,6]. The Gulf of Aqaba (Northern Red Sea) experienced rapid industrial development in the twentieth century, resulting in coral death due to elevated nitrate, phosphate and trace metal concentrations [7].

Giant clams—including the three Red Sea species *Tridacna squamosa*, *T. maxima* and the rare endemic *T. squamosina*—have photosymbiotic algae that accelerate shell growth and, like corals, require oligotrophic water [1]. Giant clams experience similar oxidative stress and bleaching as corals at high temperatures [1,8]. They are also sensitive to turbidity associated with eutrophication [9]. However, the physiological response of tridacnids to combined stresses of temperature and eutrophication is less studied, which can be remedied through investigation of their historical and modern growth in the natural laboratory of the Northern Red Sea. If the stressors harming corals in the Northern Red Sea also influence giant clams, the clams could show slower growth in the modern day. In this study, we investigate whether giant clam shell growth differed in pre-industrial times, and whether environmental and physiological changes as

recorded by shell stable isotopes ($\delta^{15}N$ and $\delta^{18}O$) can explain any observed growth changes.

The Northern Red Sea represents an opportune environment to evaluate the effects of temperature, seasonality and eutrophication on the growth of fossil and modern giant clams, as there are well-preserved Late Pleistocene and Holocene reefs exposed directly onshore [10,11] from modern fringing reefs that still contain *Tridacna*. Tridacnid growth can be benchmarked in fossil and modern specimens using sclerochronology [12], while oxygen isotope palaeothermometry can reconstruct their past and present temperature environments [13]. Nitrogen isotopes of the shell organic matrix can record changing N sources in modern and fossil specimens [14–18], as nitrate aerosols have relatively low $\delta^{15}N$ values [19] and sewage pollution very high values [20]. By comparing the growth of pre-industrial and modern *Tridacna*, we can understand how changes in nutrient availability or temperature influence shell production in this important reef organism. Quantifying their comparative growth in ancient and modern times can help understand changes in their physiology as well as the health of the reefs on which they live.

2. Methods

From June to August 2016, we collected 55 empty shells of the three Red Sea *Tridacna* species (figure 1, electronic supplementary material, Data). All collection was conducted in the surf zone with approval from local Marine Protected Area authorities (Israeli National Parks Service permit 2016/41334). Seven additional shells are believed to have been collected illegally in Northern Sinai, and were obtained from the Hebrew University of Jerusalem. We collected subfossil remains of Late Pleistocene and Holocene *Tridacna* from several sites along the Israeli and Jordanian coast (figure 1), including 10 shells surfaced during construction from the same horizon as a buried reef previously radiocarbon dated as 4500 ± 100 yr in age [10]. We pried three shells from cemented 'reef rock' at the Tur Yam site coeval with corals dated between 6800 and 5400 yr age [21]. We collected six shells from a Jordanian emerged reef platform (terrace 'R2') that contains corals of 117 000 ± 3000 yr in age [11].

We identified species with a taxonomic key previously used for Gulf of Aqaba tridacnids [22] and used scanning electron microscopy (SEM) to select shells with original crossed-lamellar aragonite for subsequent stable isotope analyses (electronic supplementary material, figure S1). More information on screening methodology may be found in the electronic supplementary material. We milled a subset of nine shells (six modern and three fossil) sequentially at 3–4 mm resolution to reconstruct seasonal $\delta^{18}O$ oscillations for palaeothermometry to calibrate growth lines (electronic supplementary material, figure S2) and collected bulk samples using a Dremel tool from the outer growth layer for determination of mean palaeotemperature. Bulk sampling averages the $\delta^{18}O$ values of increments across the multiple years of growth displayed by the majority of our studied individuals [23]. $\delta^{18}O$ values were converted to temperatures using the equation of Grossman & Ku [24], previously used in multiple *Tridacna* studies [23–27] and a seawater $\delta^{18}O$ value of 1.8‰ relative to VSMOW previously measured from the Northern Red Sea [28,29]. To measure nitrogen isotope ratios of shell organic matrix, we collected chips from near the shell margin and ground them for $\delta^{15}N$ measurement with a CE Instruments NC2500 elemental analyser interfaced to a ThermoFinnegan Delta Plus XP Isotope Ratio Mass Spectrometer. Results are reported relative to air for $\delta^{15}N$. Detailed methodological information on the preparation and measurement of $\delta^{18}O$ and $\delta^{15}N$ values may be found in the electronic supplementary material.

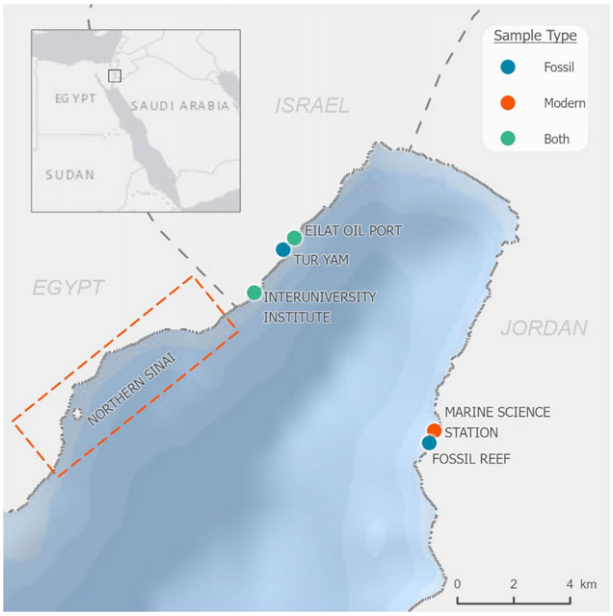

Figure 1. Map showing study localities around the Gulf of Aqaba. (Online version in colour.)

A subset of three fossil shells and two modern shells were bleached to test the influence of the removal of intercrystalline organics on measured $\delta^{15}N$ values, similar to prior studies of bivalves [30] and corals [31]. We immersed powder samples in 12% NaOCl for 4, 8 and 12 h. The solution was then centrifuged, the supernatant removed by pipet and the powder rinsed with deionized water. The procedure was repeated two additional times. The powders were left to air-dry on filter paper for 2 days before being measured for $\delta^{15}N$ values in the same fashion as mentioned above.

We assembled a subsample of shells for sclerochronological profiling (see electronic supplementary material for the procedure). Bivalve growth rates vary through ontogeny, although the majority of our collection are subadults in the linear growth phase prior to mature deceleration [25]. To control for comparison of growth among our shells, which range from 2 to 12.5 cm in height, we used two indices: the Von Bertalanffy growth constant k [32] and the related standardized growth performance index ϕ' [33]. Animals with higher k values show a faster maturation rate [34], while ϕ' is an index of growth performance specifically developed for cross-species comparisons [33]. Both are calculated using metrics such as growth rate, theoretical maximum size and other variables, and both have been used alternatively in the literature on giant clam growth [32], so we include both in our results. ϕ' was used in previous tridacnid growth databases [22,35], which allows us to assess the comparative growth of fossil and modern Red Sea tridacnids. Additional information on relevant equations to calculate k and ϕ' are available in the electronic supplementary material.

Growth rate indices were compared across species and time using one-way analyses of variance (ANOVA). Normally distributed subsets were compared with Welch's t-test and Pearson's correlation. Those which were not normally distributed as indicated by Shapiro–Wilk tests were analysed with nonparametric tests such as Wilcoxon rank sum test and Kendall correlation.

3. Results

Among the three species, *T. squamosina* showed the fastest modern growth as measured in millimetres per year (43.7), k (0.32) and ϕ' (2.0), with *T. squamosa* at intermediate rates and *T. maxima* slowest (table 1). These k values are in the range

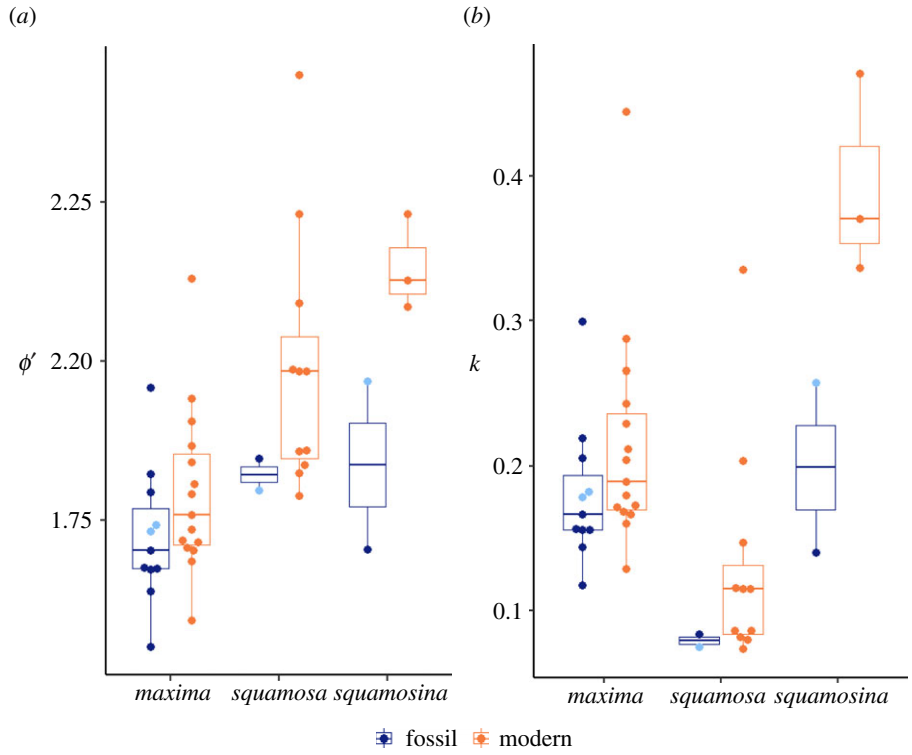

Figure 2. Fossil and modern box plot split by species for ϕ' (*a*) and Von Bertalanffy's *k* (*b*) indices. Boxes encompass the middle quartiles while the whiskers represent 1.5× interquartile range. Light blue points are Interglacial Maximum in age while dark blue points are from the Holocene. (Online version in colour.)

Table 1. Mean annual growth rates, Von Bertalanffy's *k* and phi prime values for fossil and modern giant clam populations. Standard deviations for all statistics in parentheses and italics.

species	*Tridacna maxima*		*T. squamosa*		*T. squamosina*	
age and number of specimens	fossil ($n = 11$)	modern ($n = 15$)	fossil ($n = 2$)	modern ($n = 11$)	fossil ($n = 2$)	modern ($n = 3$)
growth rate (mm yr^{-1})	23.8 (*10.2*)	26.7 (*5.7*)	20.2 (*1.4*)	28.2 (*13.1*)	31.0 (*6.0*)	52.3 (*9.4*)
k	0.18 (*0.05*)	0.21 (*0.07*)	0.08 (*0.01*)	0.13 (*0.08*)	0.20 (*0.08*)	0.39 (*0.07*)
ϕ'	1.72 (*0.11*)	1.79 (*0.13*)	1.82 (*0.035*)	1.99 (*0.20*)	1.84 (*0.19*)	2.15 (*0.075*)

known from other giant clams (though modern *T. squamosina* shows very rapid growth), while ϕ' measures are lower than other studies [22,35,36]. For all three species, modern specimens had significantly faster growth rates than fossil specimens, as measured by both *k* and ϕ' (figure 2, electronic supplementary material). In the collection, *T. maxima* is more numerous for both fossil and modern assemblages, and *T. squamosa* and *T. squamosina* are represented by only two fossil individuals.

Fossil populations have median $\delta^{15}N$ values 4.2‰ higher than modern shells (Wilcoxon rank sum test: $W = 144$, $p < 0.005$; figure 3*a*). The fossil and modern shells display high variability in N content (electronic supplementary material, figure S3) and $\delta^{15}N$ values (figure 3*a*), but there is no significant relationship between the variables (Kendall rank correlation: $\tau = -0.17$, $p = 0.86$). NaOCl treatment resulted in all samples losing over 50% of their N content after the first 4 h of treatment (electronic supplementary material, figure S4). Measured $\delta^{15}N$ declined outside of instrumental error in one treated fossil shell, but the others had differences smaller than the instrumental error.

Median organic $\delta^{13}C$ values are not significantly different between fossil and modern shells (fossil: 3.09‰, modern: 2.65‰, Wilcoxon rank sum test: $W = 194.5$, *p*-value = 0.194, electronic supplementary material, figure S5). Mean $\delta^{18}O$ is slightly lower across all modern specimens (1.11‰, $n = 26$) than those from the Holocene (1.36‰, $n = 6$), but very similar to shells from the 117 kyr Jordanian reef (1.16‰, $n = 2$, figure 3b). Overall, assuming a $\delta^{18}O_{seawater}$ value of 1.8‰, modern shells record a higher mean temperature (22.4°C) than the pooled fossil shells (21.6°C), although this difference is not significant ($t = 1.27$, d.f. = 16.63, *p*-value = 0.22; figure 3*b*).

There is a positive relationship between temperature and ϕ' across all species (Kendall rank correlation: $\tau = 0.27$, *p*-value = 0.03; figure 3*d*). The faster-growing *T. squamosa* and *T. squamosina* recorded higher temperatures, except for one shell that experienced mean temperatures above 27°C, which likely depressed its growth. There is a weak but not statistically significant negative relationship between ϕ' and $\delta^{15}N$ (Kendall correlation: $\tau = -0.153$, *p*-value = 0.297; figure 3*c*).

There is a statistically significant negative relationship between shell height and $\delta^{15}N$ (Kendall rank correlation: $\tau = -0.361$, *p*-value = 0.010, electronic supplementary material, figure S7), but not between ontogenetic age and $\delta^{15}N$ (Kendall rank correlation: $\tau = -0.263$, *p*-value = 0.115). Modern shells

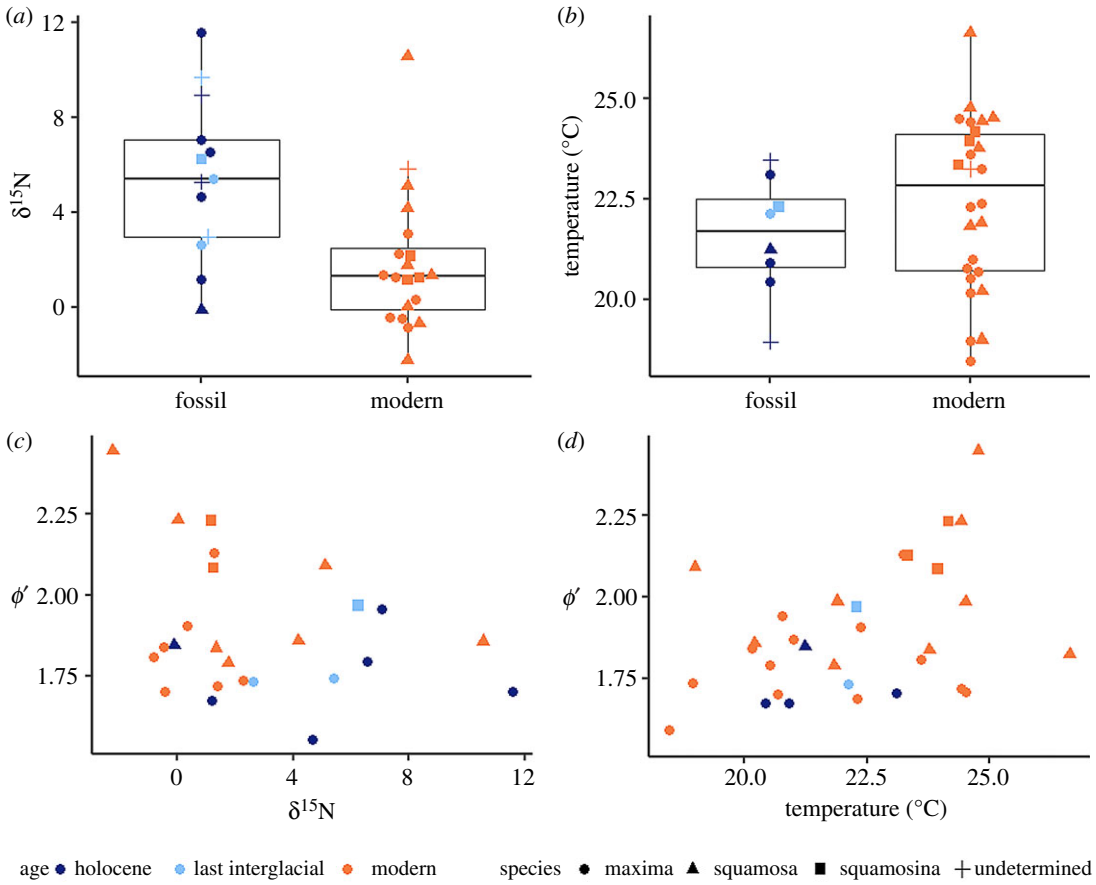

Figure 3. (*a*) Comparison of fossil and modern nitrogen isotope values. (*b*) Comparison of fossil and modern oxygen isotope palaeotemperature output. (*c*) Comparison of ϕ' and nitrogen isotope values. The relationship is not statistically significant. (*d*) Comparison of ϕ' and shell formation temperature. The relationship is statistically significant. Legend for both scatter plots at bottom. (Online version in colour.)

show a larger median shell height (6.99 cm) than fossil shells (3.93 cm), but that difference is not significant (Wilcoxon rank sum test: $W = 51$, p-value = 0.133).

4. Discussion

(a) Temperature and climate

The growth of modern *Tridacna* in the Northern Red Sea is faster compared to fossil populations as measured by linear growth rates and when scaled to ontogeny using two growth metrics. The first potential explanation for this change is temperature. Among our specimens, we found a positive correlation between growth rate and temperature, corroborating other observations of tridacnid growth [37]. These differences in mean temperature between individuals likely result from microenvironmental variability at different depths along the reefs of the Gulf of Aqaba, which can experience greater than 3°C differences between the shallow lagoon and the fore-reef [23]. Depressed growth above 27°C aligns with past observations of tridacnid thermal tolerance thresholds [8]. The Red Sea has experienced little change in mean annual SST in the late Holocene [38], and experienced around the same mean temperatures at the last interglacial [39], which may explain the lack of a statistically significant difference between the mean temperatures recorded for our fossil and modern shells. In our reconstructions, we assumed that seawater $\delta^{18}O$ was the same as the modern during the Last Interglacial and recent Holocene. This assumption will require corroboration with techniques that provide absolute temperature estimates, such as the clumped isotope approach [40], but our estimated palaeotemperatures do fall around the means of temperature timeseries produced from interglacial and late Holocene (4.6–5.75 kyr) corals in combination with a general circulation model [6]. While Red Sea seawater $\delta^{18}O$ has shifted during past salinity and eustatic changes, it is thought to have displayed similarly low values to today in the recent Holocene and last interglacial time periods [41].

Prior high-resolution coral reconstructions from the Red Sea suggested that seasonality was greater than today, with hotter summers and colder winters [6,39]. Summer monsoons also may have reached the Gulf of Aqaba in the mid-Holocene, contributing to slower historical coral growth [5], and paralleling the slower past growth in fossil tridacnids. Storms are known to disrupt giant clam growth [27]. As modern Red Sea tridacnids experience a narrow seasonal range of around 7°C [28], with diurnal variations rivalling those of seasons [42], they may grow with fewer interruptions in both summer (due to a lack of monsoons) and winter (due to milder low temperatures).

(b) Nitrogen isotope ratios and N content

Prior investigations of the influence of diagenesis on $\delta^{15}N$ values have been conducted with subfossil oysters [14,15], fish otoliths [43], and corals of Triassic [31] and Devonian age [44]. The skeletal organic matrix is thought to be more resistant to diagenetic isotopic fractionation than the surrounding

carbonate. For example, recrystallized Triassic coral skeletal regions have similar $\delta^{15}N$ values to samples of original mineralogy [31]. Oysters with reduced N content showed no change in $\delta^{15}N$ values compared to those with better preserved organic matrix [14], though this does not negate the need to ensure sample quality through techniques like SEM. $\delta^{15}N$ values can be enriched by 2‰ in heated sediments [45], but experiments conducted on organic matter in biominerals such as oyster shell and ostrich eggshell via heating did not produce changes in isotopic values [46,47]. Previous investigation of diagenetically altered photo- and chemosymbiotic bivalve shell organic matrix found strong effects on $\delta^{13}C$ values, but minimal effects on $\delta^{15}N$ [48]. Early diagenesis of surface sediments can increase $\delta^{15}N$ by approximately 2.5‰ [49], but also generally decreases $\delta^{13}C$ values due to preferential mobilization of ^{13}C [50–52]. If our shells had been influenced by the same type of degradation, we would expect a lower median $\delta^{13}C$ value for fossil shells. Instead, we saw a slightly higher $\delta^{13}C$ value in the fossil shells (electronic supplementary material, figure S5), though the difference is not statistically significant.

Intercrystalline organics are thought to be more vulnerable to diagenetic alteration than intracrystalline organics [43,52]. Previous workers used NaOCl treatment to test if oxidative removal of the intercrystalline fraction would influence the $\delta^{15}N$ of bivalve shell organic matter [30]. In a treatment of five shells, we found a loss of the majority of N in the treated samples. $\delta^{15}N$ change due to treatment varied, from no change to a decline just outside of analytical error (electronic supplementary material, figure S4). Prior workers have suggested that $\delta^{15}N$ of the intracrystalline fraction may be inherently lower [53], while others proposed it was caused by the NaOCl treatment itself [14]. Alternatively, if the intercrystalline fraction is preferentially metabolized during diagenesis, an offset could be a signal of diagenetic alteration. The very small quantities of N present after NaOCl treatment make it difficult to measure the intracrystalline fraction with adequate precision. $\delta^{15}N$ of *Tridacna* shells in tropical arid environments merits further investigation, particularly through compound-specific approaches, to determine how differing organic fractions contribute to measured $\delta^{15}N$ values.

The studied shells showed substantial variability in N content. This could reflect the great intraspecies variability observed previously in other bivalves. In organic-rich modern oyster shells, %N can vary between 0.1% and 0.5% [14]. Researchers determined that N content mostly decreased in the first few hundred years after burial in midden oysters from temperate climates [14]. A similar diagenetic mechanism could be responsible for the variability in N content displayed in our modern shells (electronic supplementary material, figure S3), which may have persisted on the seafloor for decades or longer after death. The modern shells may be in various stages of converging on the lower fossil N yields. Shells on the seafloor in tropical carbonate environments have been found to display a multi-decade residence time (median 72 years, with some persisting much longer) [54], though among our shells, precise ages are unknown. The potential multi-decade residence time of dead shells means trends within the post-industrial era cannot be quantified without an effort to date or cross-match the individual shell records.

The shells displayed a large range of $\delta^{15}N$ values, which was also observed in other studies of bivalve shell organic $\delta^{15}N$. In the non-symbiotic *Spisula solidissima*, $\delta^{15}N$ can vary as much through the ontogeny of an individual as it does for whole-shell values across a population [55]. $\delta^{15}N$ values for *Arctica islandica* shells also have high ontogenetic variability, which the researchers proposed was due to fluctuations in environmental nitrate concentration and source isotopic composition [56]. The variability across our giant clams may be partially due to high variance in the $\delta^{15}N$ values of source N in the Gulf of Aqaba [57], which is increasingly a function of seasonal delivery of nitrate aerosols [19].

This variability could be amplified by ontogenetic dynamics unique to giant clams. Because giant clams ramp up photosymbiotic nutrition as they grow [58], the animal effectively drops in trophic level upon reaching maturity. This could lead to larger giant clams displaying lower $\delta^{15}N$ values than smaller clams still reliant on filter-feeding for most of their nutrition. There is indeed a significant negative relationship between shell height and $\delta^{15}N$ among our specimens (electronic supplementary material, figure S7). Within the same size classes of shells, fossil shells still show higher $\delta^{15}N$ than modern ones (electronic supplementary material, figure S7), suggesting that the change observed between fossil and modern shells is independent of any potential size effect. Regardless, more research is needed into how $\delta^{15}N$ and N content vary through giant clam ontogeny, and how those factors relate to their degree of symbiosis at differing life stages.

(c) Nitrate fertilization: physiological and ecosystem-wide effects

Tridacnids ingest ammonia and nitrate to support photosynthesis by their endosymbionts, which accelerates shell growth [59,60]. The development of fish farms in the Gulf of Aqaba slowed coral growth [7], but an influx of ^{15}N-enriched fish waste likely cannot explain growth patterns in *Tridacna*, as modern shell organic matrix $\delta^{15}N$ values are lower than pre-industrial values. In the western Pacific, increased monsoon activity has led to a decline in $\delta^{15}N$ records from coral skeletons, and an increase in seasonal variability [61]. Such dynamics are not applicable to the Red Sea giant clams, which have experienced declining monsoon activity since pre-industrial times [5]. However, the modern Red Sea experiences higher N supply due to anthropogenic nitrate aerosol deposition, which accounts for up to 35% of the dissolved inorganic N delivered during summer months [62]. These aerosols are depleted in ^{15}N, with a mean $\delta^{15}N$ value of −2.6‰, reaching as low as −6.9‰ in the winter [19]. Modern tridacnid shell organic matrix displays lower $\delta^{15}N$ values than those found in historical specimens, consistent with an aerosol nitrate fertilization effect.

While the specimens showed a negative correlation between growth and $\delta^{15}N$ which would be expected if fertilization by isotopically light nitrate aerosols were at work (figure 3*c*), the relationship is not statistically significant. This is perhaps unsurprising, as tridacnid growth integrates numerous competing factors related to differing N sources [60]. If the whole-shell organic matrix did not record the entire year's integrated $\delta^{15}N$ equally, since it arrived as intermittent deliveries of dust and aerosols, the degree of correlation between shell growth and $\delta^{15}N$ would be reduced. Factors in addition to symbiont fertilization could be at play, as growth increased in the modern specimens for all three species, including the more heterotrophic *T. squamosa*. In Chesapeake Bay, the growth of oysters accelerated following the rise of pre-industrial anthropogenic eutrophication [63]. Tridacnids could grow more

quickly in the Gulf of Aqaba if phytoplankton food is more readily available, particularly in low-productivity summer months. Heterotrophic nutrition makes up 30% of incoming N even in the highly photosymbiotic *T. gigas* [60].

$\delta^{15}N$ values also record the degree of N utilization in an environment. Water from plankton cultures with a N excess shows lower $\delta^{15}N$ values compared to those with nitrate drawdown [64]. In the Red Sea, lower $\delta^{15}N$ values could be a response to greater modern nitrate supply resulting in a lower degree of consumption of the nitrate pool, rather than a signal of the source N itself. Additionally, corals have been found to record lower skeletal $\delta^{15}N$ due to an increase in N fixation resulting from fertilization of phytoplankton by phosphorus discharge [65]. The Gulf of Aqaba is ringed by phosphate mining operations which could represent a relevant source of phosphate pollution not present in historic times [7]. However, phosphate has complicated feedbacks on tridacnid growth, with conflicting results depending on its pairing with nitrate [59,60]. More research into historical phosphate concentration in the Gulf of Aqaba could help disentangle these interacting mechanisms and how they manifest in the growth of photosymbiotic animals.

5. Conclusion

The resilience of giant clams in the face of environmental stresses like climate change and pollution is poorly known relative to other photosymbiotic groups. In the Northern Red Sea, modern giant clams are growing more quickly than in the past, which may be related to decreased seasonality and increased nitrate availability. It is important to caution that our data cannot determine if tridacnid growth has changed within the 1970–2020 period of reduced coral growth, and accelerated growth does not mean that the giant clams have improved fitness or overall health. In fertilization studies of giant clams, shell density and the orderliness of crystal fabrics both declined as shell extension rate accelerated [59]. While the finding that the clams reach mature size more quickly may seem encouraging for their survival, more investigation is needed to confirm whether faster-growing tridacnids have changes in resistance to crushing predation, reproductive capacity and other fitness markers. In corals, some individuals show growth acceleration due to eutrophication even as the broader reef experiences net erosion [66]. Similarly, the acceleration of *Tridacna* growth will not be a boon for their survival if the reefs they depend on are harmed. Nevertheless, giant clam shells have great potential as reef archives with value for the understanding of broader reef health, particularly if aggregated across localities to reconstruct reef 'isoscapes' [67,68]. The shell records of these filtering reef sentinels could shed light on the comparative health of other reef ecosystems. The trends observed in their growth are evidence of the variable responses that different photosymbiotic reef taxa may exhibit to anthropogenic environmental stress.

Ethics. All shells were collected with permission and supervision of relevant environmental authorities in Israel (permit no. 2016/41334) and Jordan.

Data accessibility. All data are available in the electronic supplementary material files [69] and from the Dryad Digital Repository: https://doi.org/10.7291/D1CM20 [70].

Authors' contributions. D.K.: conceptualization, data curation, formal analysis, investigation, methodology, visualization, writing—original draft, writing—review and editing; T.A.-N.: investigation, project administration, resources, supervision; M.C.: conceptualization, formal analysis, investigation, project administration, resources, supervision, writing—review and editing.

All authors gave final approval for publication and agreed to be held accountable for the work performed therein.

Competing interests. The authors state that there is no conflict of interest.

Funding. Funding was provided by the UCSC Casey Moore Fund, AMNH Lerner-Grey Foundation, Myers Oceanographic Trust and NSF Coastal IRES programme.

Acknowledgements. We thank Colin Carney and Dyke Andreasen at the UCSC Stable Isotope Laboratory and Tom Yuzhvinsky at the W.M. Keck Center for Nanoscale Optofluidics. Adina Paytan, Moty Ohevia, Michele Markowitz, Karen Petersen and Noam Baharav assisted with fieldwork. Henk Mienis, Muki Shpigel and Yonathan Shaked provided access to specimens and advice on localities. The Interuniversity Institute in Eilat provided access to work resources and their protected reef. Asaph Zvuloni (Israel Nature and Parks Authority) supervised the collection. Dana Shultz created figure 1. Paul Koch, James Zachos and Kristy Kroeker provided comments and suggestions for the manuscript.

References

1. Neo ML *et al.* 1996 Giant clams (Bivalvia: Cardiidae: Tridacninae): a comprehensive update of species and their distribution, current threats and conservation status. *Oceanogr. Mar. Biol. Annu. Rev.* **55**, 87–387. (doi:10.1201/b21944-5)
2. Dubinsky Z, Stambler N. 1996 Marine pollution and coral reefs. *Glob. Change Biol.* **2**, 511–526. (doi:10.1111/j.1365-2486.1996.tb00064.x)
3. Cantin NE, Cohen AL, Karnauskas KB, Tarrant AM, McCorkle DC. 2010 Ocean warming slows coral growth in the Central Red Sea. *Science* **329**, 322–325. (doi:10.1126/science.1190182)
4. Hume BCC, Voolstra CR, Arif C, D'Angelo C, Burt JA, Eyal G, Loya Y, Wiedenmann J. 2016 Ancestral genetic diversity associated with the rapid spread of stress-tolerant coral symbionts in response to Holocene climate change. *Proc. Natl Acad. Sci. USA* **113**, 4416–4421. (doi:10.1073/pnas.1601910113)
5. Moustafa Y, Pätzold J, Loya Y, Wefer G. 2000 Mid-Holocene stable isotope record of corals from the northern Red Sea. *Int. J. Earth Sci.* **88**, 742–751. (doi:10.1007/s005310050302)
6. Felis T, Lohmann G, Kuhnert H, Lorenz SJ, Scholz D, Pätzold J, Al-Rousan SA, Al-Moghrabi SM. 2004 Increased seasonality in Middle East temperatures during the last interglacial period. *Nature* **429**, 164–168. (doi:10.1038/nature02546)
7. Loya Y. 2004 The coral reefs of eilat—past, present and future: three decades of coral community structure studies. In *Coral health and disease* (eds E Rosenberg, Y Loya), pp. 1–34. Berlin, Germany: Springer.
8. Schwartzmann C, Durrieu G, Sow M, Ciret P, Lazareth CE, Massabuau J-C. 2011 In situ giant clam growth rate behavior in relation to temperature: a one-year coupled study of high-frequency noninvasive valvometry and sclerochronology. *Limnol. Oceanogr.* **56**, 1940–1951. (doi:10.4319/lo.2011.56.5.1940)
9. Hean RL, Cacho OJ. 2003 A growth model for giant clams *Tridacna crocea* and *T. derasa*. *Ecol. Model.* **163**, 87–100. (doi:10.1016/S0304-3800(02)00400-3)
10. Shaked Y, Lazar B, Marco S, Stein M, Agnon A. 2011 Late Holocene events that shaped the shoreline at the northern Gulf of Aqaba recorded by a buried fossil reef. *Isr. J. Earth Sci.* **58**, 355–368. (doi:10.1560/IJES.58.3-4.355)

11. Yehudai M, Lazar B, Bar N, Kiro Y, Agnon A, Shaked Y, Stein M. 2017 U–Th dating of calcite corals from the Gulf of Aqaba. *Geochim. Cosmochim. Acta* **198**, 285–298. (doi:10.1016/j.gca.2016.11.005)
12. Gannon ME, Pérez-Huerta A, Aharon P, Street SC. 2017 A biomineralization study of the Indo-Pacific giant clam *Tridacna gigas*. *Coral Reefs* **36**, 503–517. (doi:10.1007/s00338-016-1538-5)
13. Aharon P. 1991 Recorders of reef environment histories: stable isotopes in corals, giant clams, and calcareous algae. *Coral Reefs* **10**, 71–90. (doi:10.1007/BF00571826)
14. Darrow ES, Carmichael RH, Andrus CFT, Jackson HE. 2017 From middens to modern estuaries, oyster shells sequester source-specific nitrogen. *Geochim. Cosmochim. Acta* **202**, 39–56. (doi:10.1016/j.gca.2016.12.023)
15. Black HD, Andrus CFT, Lambert WJ, Rick TC, Gillikin DP. 2017 δ^{15}N values in *Crassostrea virginica* shells provides early direct evidence for nitrogen loading to Chesapeake Bay. *Sci. Rep.* **7**, 44241. (doi:10.1038/srep44241)
16. Versteegh EAA, Gillikin DP, Dehairs F. 2011 Analysis of δ^{15}N values in mollusk shell organic matrix by elemental analysis/isotope ratio mass spectrometry without acidification: an evaluation and effects of long-term preservation. *Rapid Commun. Mass Spectrom.* **25**, 675–680. (doi:10.1002/rcm.4905)
17. O'Donnell TH, Macko SA, Chou J, Davis-Hartten KL, Wehmiller JF. 2003 Analysis of δ^{13}C, δ^{15}N, and δ^{34}S in organic matter from the biominerals of modern and fossil *Mercenaria* spp. *Org. Geochem.* **34**, 165–183. (doi:10.1016/S0146-6380(02)00160-2)
18. Graniero LE, Gillikin DP, Surge D, Kelemen Z, Bouillon S. 2021 Assessing δ^{15}N values in the carbonate-bound organic matrix and periostracum of bivalve shells as environmental archives. *Palaeogeogr. Palaeoclimatol. Palaeoecol.* **564**, 110108. (doi:10.1016/j.palaeo.2020.110108)
19. Wankel SD, Chen Y, Kendall C, Post AF, Paytan A. 2010 Sources of aerosol nitrate to the Gulf of Aqaba: evidence from δ^{15}N and δ^{18}O of nitrate and trace metal chemistry. *Mar. Chem.* **120**, 90–99. (doi:10.1016/j.marchem.2009.01.013)
20. Carmichael RH, Hattenrath T, Valiela I, Michener RH. 2008 Nitrogen stable isotopes in the shell of *Mercenaria mercenaria* trace wastewater inputs from watersheds to estuarine ecosystems. *Aquat. Biol.* **4**, 99–111. (doi:10.3354/ab00106)
21. Weil N. 2008 Holocene coral reefs evolution in the Gulf of Eilat: Terraces, sea-levels and growth patterns. Masters thesis, Hebrew University of Jerusalem, Jerusalem.
22. Roa-Quiaoit HAF. 2005 The ecology and culture of giant clams (Tridacnidae) in the Jordanian sector of the Gulf of Aqaba, Red Sea. PhD thesis. Univeristy of Bremen, Bremen, Germany. See https://media.suub.uni-bremen.de/handle/elib/2141.
23. Killam D, Thomas R, Al-Najjar T, Clapham M. 2020 Interspecific and intrashell stable isotope variation among the Red Sea giant clams. *Geochem. Geophys. Geosyst.* **21**, e2019G. (doi:10.1029/2019GC008669)
24. Grossman EL, Ku T-L. 1986 Oxygen and carbon isotope fractionation in biogenic aragonite: temperature effects. *Chem. Geol. Isot. Geosci. Sect.* **59**, 59–74. (doi:10.1016/0168-9622(86)90057-6)
25. Romanek CS, Jones DS, Williams DF, Krantz DE, Radtke R. 1987 Stable isotopic investigation of physiological and environmental changes recorded in shell carbonate from the giant clam *Tridacna maxima*. *Mar. Biol.* **94**, 385–393. (doi:10.1007/BF00428244)
26. Elliot M, Welsh K, Chilcott C, McCulloch M, Chappell J, Ayling B. 2009 Profiles of trace elements and stable isotopes derived from giant long-lived *Tridacna gigas* bivalves: potential applications in paleoclimate studies. *Palaeogeogr. Palaeoclimatol. Palaeoecol.* **280**, 132–142. (doi:10.1016/j.palaeo.2009.06.007)
27. Komagoe T, Watanabe T, Shirai K, Yamazaki A, Uematu M. 2018 Geochemical and microstructural signals in giant clam *Tridacna maxima* recorded typhoon events at Okinotori Island. *Jpn. J. Geophys. Res. Biogeosci.* **123**, 1460–1474. (doi:10.1029/2017JG004082)
28. Al-Rousan S, Al-Moghrabi S, Pätzold J, Wefer G. 2003 Stable oxygen isotopes in *Porites* corals monitor weekly temperature variations in the northern Gulf of Aqaba, Red Sea. *Coral Reefs* **22**, 346–356. (doi:10.1007/s00338-003-0321-6)
29. Andrié C, Merlivat L. 1989 Contribution des données isotopiques de deutérium, oxygène-18, hélium-3 et tritium, à l'étude de la circulation de la Mer Rouge. *Oceanol. Acta* **12**, 165–174.
30. Gillikin DP, Lorrain A, Jolivet A, Kelemen Z, Chauvaud L, Bouillon S. 2017 High-resolution nitrogen stable isotope sclerochronology of bivalve shell carbonate-bound organics. *Geochim. Cosmochim. Acta* **200**, 55–66. (doi:10.1016/j.gca.2016.12.008)
31. Tornabene C, Martindale RC, Wang XT, Schaller MF. 2017 Detecting photosymbiosis in fossil scleractinian corals. *Sci. Rep.* **7**, 9465. (doi:10.1038/s41598-017-09008-4)
32. Munro JL. 1982 Estimation of the parameters of the von Bertalanffy growth equation from recapture data at variable time intervals. *ICES J Mar Sci.* **40**, 199–200. (doi:10.1093/icesjms/40.2.199)
33. Pauly D, Munro JL. 1984 Once more on the comparison of growth in fish and invertebrates. Fishbyte **2**, 1–21.
34. Moss DK, Ivany LC, Judd EJ, Cummings PW, Bearden CE, Kim W-J, Artruc EG, Driscoll JR. 2016 Lifespan, growth rate, and body size across latitude in marine Bivalvia, with implications for Phanerozoic evolution. *Proc. R. Soc. B* **283**, 20161364. (doi:10.1098/rspb.2016.1364)
35. Vakily JM. 1992 *Determination and comparison of bivalve growth, with emphasis on Thailand and other tropical areas*, vol. 801. Manila, Philippines: WorldFish.
36. Mohammed TAA, Mohamed MH, Zamzamy RM, Mahmoud MAM. 2019 Growth rates of the giant clam *Tridacna maxima* (Röding, 1798) reared in cages in the Egyptian Red Sea. *Egypt. J. Aquat. Res.* **45**, 67–73. (doi:10.1016/j.ejar.2019.02.003)
37. Wynsberge SV, Andréfouët S, Gaertner-Mazouni N, Wabnitz CCC, Menoud M, Moullac GL, Levy P, Gilbert A, Remoissenet G. 2017 Growth, survival and reproduction of the giant clam *Tridacna maxima* (Röding 1798, Bivalvia) in two contrasting lagoons in French Polynesia. *PLoS ONE* **12**, e0170565. (doi:10.1371/journal.pone.0170565)
38. Felis T, Pätzold J, Loya Y, Fine M, Nawar AH, Wefer G. 2000 A coral oxygen isotope record from the northern Red Sea documenting NAO, ENSO, and North Pacific teleconnections on Middle East climate variability since the year 1750. *Paleoceanography* **15**, 679–694. (doi:10.1029/1999PA000477)
39. Hoffman JS, Clark PU, Parnell AC, He F. 2017 Regional and global sea-surface temperatures during the last interglaciation. *Science* **355**, 276–279. (doi:10.1126/science.aai8464)
40. Henkes GA, Passey BH, Wanamaker AD, Grossman EL, Ambrose WG, Carroll ML. 2013 Carbonate clumped isotope compositions of modern marine mollusk and brachiopod shells. *Geochim. Cosmochim. Acta* **106**, 307–325. (doi:10.1016/j.gca.2012.12.020)
41. Reiss Z, Luz B, Almogi-Labin A, Halicz E, Winter A, Wolf M, Ross DA. 1980 Late quaternary paleoceanography of the Gulf of Aqaba (Elat), Red Sea 1. *Quat. Res.* **14**, 294–308. (doi:10.1016/0033-5894(80)90013-7)
42. Edwards AJ. 2013 *Red Sea*. Oxford, UK: Elsevier.
43. Lueders-Dumont JA, Wang XT, Jensen OP, Sigman DM, Ward BB. 2018 Nitrogen isotopic analysis of carbonate-bound organic matter in modern and fossil fish otoliths. *Geochim. Cosmochim. Acta* **224**, 200–222. (doi:10.1016/j.gca.2018.01.001)
44. Hickey AN, Junium CK, Uveges BT, Ivany LC, Martindale RC. 2017 Carbon and nitrogen isotopic analysis of coral-associated nitrogen in rugose corals of the Middle Devonian, implications for paleoecology and paleoceanography. In *AGU Fall Meeting Abstracts. New Orleans, Louisiana. 11 December*. Washington, DC: American Geophysical Union.
45. Qian Y, Engel MH, Macko SA. 1992 Stable isotope fractionation of biomonomers during protokerogen formation. *Chem. Geol. Isot. Geosci. Sect.* **101**, 201–210. (doi:10.1016/0009-2541(92)90002-M)
46. Johnson BJ, Fogel ML, Miller GH. 1998 Stable isotopes in modern ostrich eggshell: a calibration for paleoenvironmental applications in semi-arid regions of southern Africa. *Geochim. Cosmochim. Acta* **62**, 2451–2461. (doi:10.1016/S0016-7037(98)00175-6)
47. Black HD. 2014 Δ^{15}N in mollusk shells as a potential paleoenvironmental proxy for nitrogen loading in Chesapeake Bay. Masters thesis, The University of Alabama. Tuscaloosa, Alabama.
48. Dreier A, Loh W, Blumenberg M, Thiel V, Hause-Reitner D, Hoppert M. 2014 The isotopic biosignatures of photo- vs. thiotrophic bivalves: are they preserved in fossil shells? *Geobiology* **12**, 406–423. (doi:10.1111/gbi.12093)

49. Robinson RS *et al.* 2012 A review of nitrogen isotopic alteration in marine sediments. *Paleoceanography* **27**, PA4203. (doi:10.1029/2012PA002321)
50. Freudenthal T, Wagner T, Wenzhöfer F, Zabel M, Wefer G. 2001 Early diagenesis of organic matter from sediments of the eastern subtropical Atlantic: evidence from stable nitrogen and carbon isotopes. *Geochim. Cosmochim. Acta* **65**, 1795–1808. (doi:10.1016/S0016-7037(01)00554-3)
51. Spiker EC, Hatcher PG. 1984 Carbon isotope fractionation of sapropelic organic matter during early diagenesis. *Org. Geochem.* **5**, 283–290. (doi:10.1016/0146-6380(84)90016-0)
52. Robbins LL, Ostrom PH. 1995 Molecular isotopic and biochemical evidence of the origin and diagenesis of shell organic material. *Geology* **23**, 345–348. (doi:10.1130/0091-7613(1995)023<0345:MIABEO>2.3.CO;2)
53. Pape E, Gill FL, Newton RJ, Little CTS, Abbott GD. 2018 Methodological comparison for the isolation of shell-bound organic matter for carbon, nitrogen and sulfur stable isotope analysis. *Chem. Geol.* **493**, 87–99. (doi:10.1016/j.chemgeo.2018.05.028)
54. Kidwell SM, Best MMR, Kaufman DS. 2005 Taphonomic trade-offs in tropical marine death assemblages: differential time averaging, shell loss, and probable bias in siliciclastic vs. carbonate facies. *Geology* **33**, 729–732. (doi:10.1130/G21607.1)
55. Das S, Judd EJ, Uveges BT, Ivany LC, Junium CK. 2021 Variation in δ^{15}N from shell-associated organic matter in bivalves: implications for studies of modern and fossil ecosystems. *Palaeogeogr. Palaeoclimatol. Palaeoecol.* **562**, 110076. (doi:10.1016/j.palaeo.2020.110076)
56. Whitney NM, Johnson BJ, Dostie PT, Luzier K, Wanamaker AD. 2019 Paired bulk organic and individual amino acid δ^{15}N analyses of bivalve shell periostracum: a paleoceanographic proxy for water source variability and nitrogen cycling processes. *Geochim. Cosmochim. Acta* **254**, 67–85. (doi:10.1016/j.gca.2019.03.019)
57. Aberle N, Hansen T, Boettger-Schnack R, Burmeister A, Post AF, Sommer U. 2010 Differential routing of 'new' nitrogen toward higher trophic levels within the marine food web of the Gulf of Aqaba, Northern Red Sea. *Mar. Biol.* **157**, 157–169. (doi:10.1007/s00227-009-1306-y)
58. Yau AJ-Y, Fan T-Y. 2012 Size-dependent photosynthetic performance in the giant clam *Tridacna maxima*, a mixotrophic marine bivalve. *Mar. Biol.* **159**, 65–75. (doi:10.1007/s00227-011-1790-8)
59. Belda CA, Cuff C, Yellowlees D. 1993 Modification of shell formation in the giant clam *Tridacna gigas* at elevated nutrient levels in sea water. *Mar. Biol.* **117**, 251–257. (doi:10.1007/BF00345670)
60. Fitt WK, Rees TAV, Braley RD, Lucas JS, Yellowlees D. 1993 Nitrogen flux in giant clams: size-dependency and relationship to zooxanthellae density and clam biomass in the uptake of dissolved inorganic nitrogen. *Mar. Biol.* **117**, 381–386.
61. Ren H, Chen Y-C, Wang XT, Wong GTF, Cohen AL, DeCarlo TM, Weigand MA, Mii HS, Sigman DM. 2017 21st-century rise in anthropogenic nitrogen deposition on a remote coral reef. *Science* **356**, 749–752. (doi:10.1126/science.aal3869)
62. Chen Y, Mills S, Street J, Golan D, Post A, Jacobson M, Paytan A. 2007 Estimates of atmospheric dry deposition and associated input of nutrients to Gulf of Aqaba seawater. *J. Geophys. Res. Atmos.* **112**, D04309. (doi:10.1029/2006JD007858)
63. Kirby MX, Miller HM. 2005 Response of a benthic suspension feeder (*Crassostrea virginica* Gmelin) to three centuries of anthropogenic eutrophication in Chesapeake Bay. *Estuar. Coast Shelf Sci.* **62**, 679–689. (doi:10.1016/j.ecss.2004.10.004)
64. Waser NaD, Harrison PJ, Nielsen B, Calvert SE, Turpin DH. 1998 Nitrogen isotope fractionation during the uptake and assimilation of nitrate, nitrite, ammonium, and urea by a marine diatom. *Limnol. Oceanogr.* **43**, 215–224. (doi:10.4319/lo.1998.43.2.0215)
65. Erler DV, Farid HT, Glaze TD, Carlson-Perret NL, Lough JM. 2020 Coral skeletons reveal the history of nitrogen cycling in the coastal Great Barrier Reef. *Nat. Commun.* **11**, 1–8. (doi:10.1038/s41467-020-15278-w)
66. Edinger EN, Limmon GV, Jompa J, Widjatmoko W, Heikoop JM, Risk MJ. 2000 Normal coral growth rates on dying reefs: are coral growth rates good indicators of reef health? *Mar. Pollut. Bull.* **40**, 404–425. (doi:10.1016/S0025-326X(99)00237-4)
67. Thibault M, Duprey N, Gillikin DP, Thébault J, Douillet P, Chauvaud L, Amice E, Munaron JM, Lorrain A. 2020 Bivalve δ^{15}N isoscapes provide a baseline for urban nitrogen footprint at the edge of a World Heritage coral reef. *Mar. Pollut. Bull.* **152**, 110870. (doi:10.1016/j.marpolbul.2019.110870)
68. Fujii T, Tanaka Y, Maki K, Saotome N, Morimoto N, Watanabe A, Miyajima T. 2020 Organic carbon and nitrogen isoscapes of reef corals and algal symbionts: relative influences of environmental gradients and heterotrophy. *Microorganisms* **8**, 1221. (doi:10.3390/microorganisms8081221)
69. Killam D, Al-Najjar T, Clapham M. 2021 Giant clam growth in the Gulf of Aqaba is accelerated compared to fossil populations. FigShare.
70. Killam D, Al-Najjar T, Clapham M. 2021 Data from: Giant clam growth in the Gulf of Aqaba is accelerated compared to fossil populations. Dryad Digital Repository. (https://doi.org/10.7291/D1CM20)